Differential control of human Treg and effector T cells in tumor immunity by Fc-engineered anti–CTLA-4 antibody

Danbee Ha[a,b], Atsushi Tanaka[a], Tatsuya Kibayashi[a,c], Atsushi Tanemura[d], Daisuke Sugiyama[a,1], James Badger Wing[a], Ee Lyn Lim[a], Karen Wei Weng Teng[e], Dennis Adeegbe[a,2], Evan W. Newell[e], Ichiro Katayama[d], Hiroyoshi Nishikawa[a,1,3], and Shimon Sakaguchi[a,b,4]

[a]Experimental Immunology, Immunology Frontier Research Center, Osaka University, 565-0871 Osaka, Japan; [b]Laboratory of Experimental Immunology, Department of Regeneration Science and Engineering, Institute for Frontier Life and Medical Sciences, Kyoto University, 606-8507 Kyoto, Japan; [c]Research Division, Chugai Pharmaceutical Co., Ltd., 247-8530 Kanagawa, Japan; [d]Department of Dermatology, Graduate School of Medicine, Osaka University, 565-0871 Osaka, Japan; and [e]Agency for Science, Technology and Research, Singapore Immunology Network, 138632 Singapore

Contributed by Shimon Sakaguchi, November 23, 2018 (sent for review July 19, 2018; reviewed by Miyuki Azuma and Sergio A. Quezada)

Anti–CTLA-4 mAb is efficacious in enhancing tumor immunity in humans. CTLA-4 is expressed by conventional T cells upon activation and by naturally occurring FOXP3$^+$CD4$^+$ Treg cells constitutively, raising a question of how anti–CTLA-4 mAb can differentially control these functionally opposing T cell populations in tumor immunity. Here we show that FOXP3^{high} potently suppressive effector Treg cells were abundant in melanoma tissues, expressing CTLA-4 at higher levels than tumor-infiltrating CD8$^+$ T cells. Upon in vitro tumor-antigen stimulation of peripheral blood mononuclear cells from healthy individuals or melanoma patients, Fc-region–modified anti–CTLA-4 mAb with high antibody-dependent cell-mediated cytotoxicity (ADCC) and cellular phagocytosis (ADCP) activity selectively depleted CTLA-4$^+$FOXP3$^+$ Treg cells and consequently expanded tumor-antigen–specific CD8$^+$T cells. Importantly, the expansion occurred only when antigen stimulation was delayed several days from the antibody treatment to spare CTLA-4$^+$ activated effector CD8$^+$T cells from mAb-mediated killing. Similarly, in tumor-bearing mice, high-ADCC/ADCP anti–CTLA-4 mAb treatment with delayed tumor-antigen vaccination significantly prolonged their survival and markedly elevated cytokine production by tumor-infiltrating CD8$^+$ T cells, whereas antibody treatment concurrent with vaccination did not. Anti–CTLA-4 mAb modified to exhibit a lesser or no Fc-binding activity failed to show such timing-dependent in vitro and in vivo immune enhancement. Thus, high ADCC anti–CTLA-4 mAb is able to selectively deplete effector Treg cells and evoke tumor immunity depending on the CTLA-4–expressing status of effector CD8$^+$ T cells. These findings are instrumental in designing cancer immunotherapy with mAbs targeting the molecules commonly expressed by FOXP3$^+$ Treg cells and tumor-reactive effector T cells.

regulatory T cells | CTLA-4 | FOXP3 | cancer immunotherapy | antibody-dependent cell-mediated cytotoxicity

Naturally occurring CD25$^+$CD4$^+$ Treg cells, which express the transcription factor FOXP3, play indispensable roles in the maintenance of immunological self-tolerance and homeostasis (1). However, they also hinder effective immune responses against tumor cells arising from self, as illustrated by the findings that mouse tumors can be eradicated simply by depletion of Treg cells (2–5). In humans, there is accumulating evidence for abundant infiltration of Treg cells into various tumor tissues (6–8), and a significant correlation between Treg infiltration and poor prognosis in various types of cancers (9). Control of Treg cells in tumor tissues is therefore likely to be one promising way for evoking effective tumor immunity in cancer patients.

Human FOXP3-expressing CD4$^+$ T cells are heterogeneous in function, including Treg cells and nonsuppressive conventional T cells. They can be fractionated into three subpopulations by their different expression levels of FOXP3 and CD45RA (10) (Fig. 1*A*): (*i*) CD45RA$^+$FOXP3^{lo} naïve/resting Treg cells [Fraction (Fr). I]; (*ii*) CD45RA$^-$FOXP3^{hi} effector Treg (eTreg) cells (Fr. II), which are terminally differentiated and highly suppressive; and (*iii*) CD45RA$^-$FOXP3^{lo} non-Treg cells (Fr. III), which lack suppressive activity and are capable of secreting proinflammatory cytokines. Upon antigenic stimulation, Fr. I naïve Treg cells differentiate into Fr. II eTreg cells, which highly express CTLA-4 (10). Although most cells in Fr. III are non-Treg cells and do not differentiate into Fr. II eTreg cells, a circulating subset of T-follicular regulatory cells, which are CXCR5$^+$CD45RA$^-$, is included in Fr. III (11), indicating heterogeneity of the Fr. III population. In contrast, with the presence of these three FOXP3$^+$ populations in the blood, the majority of tumors show predominant infiltration of eTreg cells, which appear to be suppressing effective antitumor immune responses in cancer patients (12). These findings suggest that depletion/reduction of eTreg cells in tumors and regional lymph nodes

IMMUNOLOGY AND INFLAMMATION

Significance

Anti–CTLA-4 mAb is able to augment tumor immunity despite CTLA-4 expression by functionally opposing T cell populations: activated effector T (Teff) cells and FOXP3$^+$CD4$^+$ Treg cells. Here we show that anti–CTLA-4 mAb engineered to be cytotoxic depleted Treg cells effectively in vitro in humans and in vivo in mice. It expanded antigen-specific CD8$^+$ Teff cells when tumor-antigen stimulation was delayed several days to protect them from killing by the mAb. Anti–CTLA-4 mAb modified to exhibit a lesser or no cell-depleting activity failed to show such effects. This strategy of differentially controlling Treg and Teff cells by cytotoxic anti–CTLA-4 mAb to evoke effective tumor immunity will help in designing cancer immunotherapy targeting other molecules commonly expressed by Treg and Teff cells.

Author contributions: D.H., A. Tanaka, H.N., and S.S. designed research; D.H., A. Tanaka, T.K., A. Tanemura, D.S., J.B.W., E.L.L., K.W.W.T., D.A., and I.K. performed research; A. Tanemura contributed new reagents/analytic tools; D.H., A. Tanaka, T.K., D.S., D.A., E.W.N., I.K., H.N., and S.S. analyzed data; and D.H., A. Tanaka, and S.S. wrote the paper.

Reviewers: M.A., Tokyo Medical and Dental University; and S.A.Q., University College London.

Conflict of interest statement: H.N. received a research grant from Bristol Myers Squibb. S.S. received a research grant from Chugai Pharmaceutical Co., Ltd. T.K. is employed by Chugai Pharmaceutical Co., Ltd. which provided some of the antibodies used in this study.

Published under the PNAS license.

[1]Present address: Department of Immunology, Graduate School of Medicine, Nagoya University, 466-8550 Nagoya, Japan.

[2]Present address: Department of Immunology, Moffitt Cancer Center, Tampa, FL 33612.

[3]Present address: Division of Cancer Immunology, Exploratory Oncology Research & Clinical Trial Center, National Cancer Center, 277-8577 Kashiwa, Japan.

[4]To whom correspondence should be addressed. Email: shimon@ifrec.osaka-u.ac.jp.

This article contains supporting information online at www.pnas.org/lookup/suppl/doi:10.1073/pnas.1812186116/-/DCSupplemental.

Published online December 26, 2018.

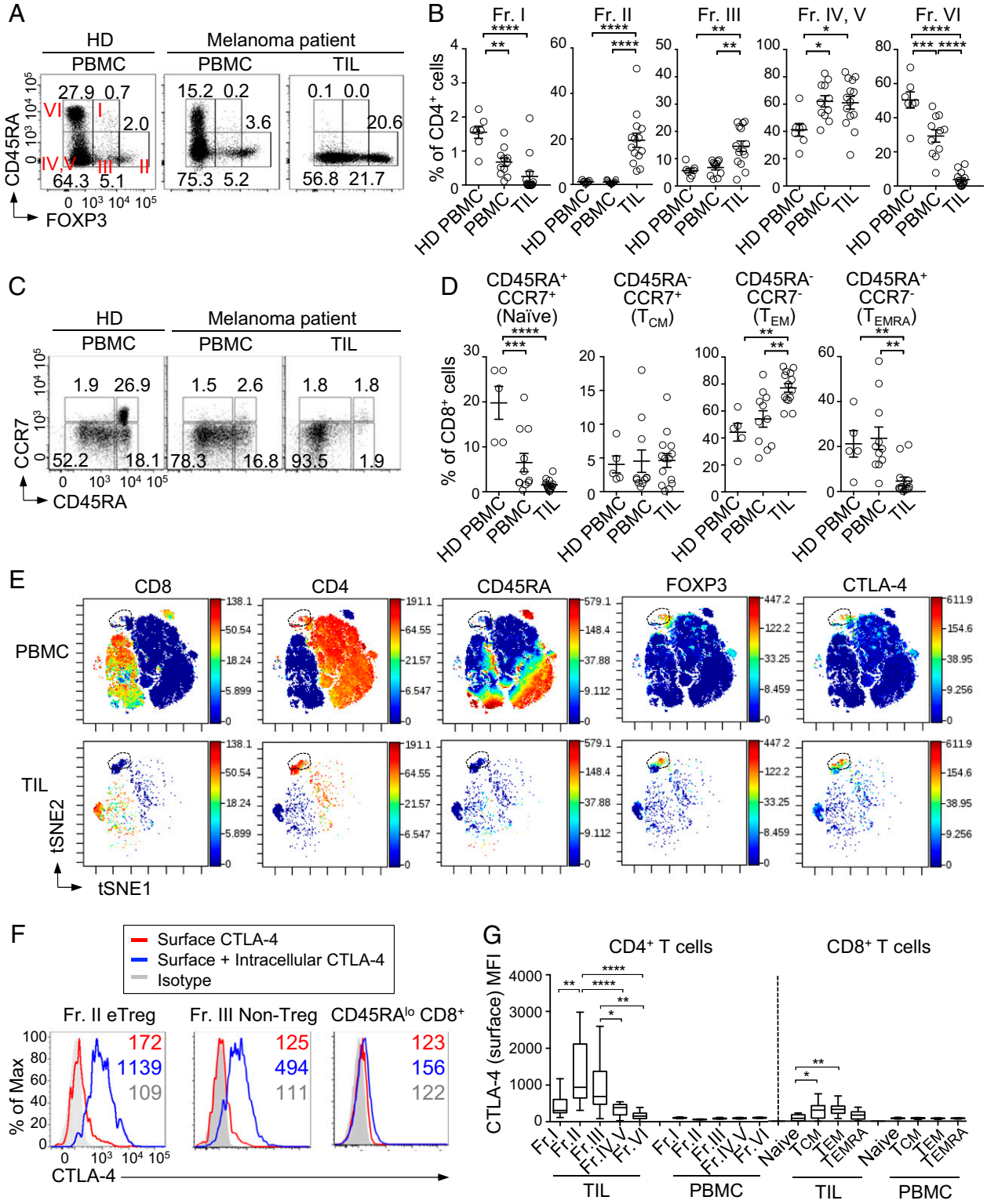

Fig. 1. Preferential CTLA-4 expression by FOXP3^{hi} eTreg cells in melanoma tissue. (*A* and *B*) Representative plots of CD4^{+} T cell staining (*A*) and frequencies of each fraction (*B*). PBMCs of healthy donors (HD, $n = 5$), and PBMCs and TILs of melanoma patients ($n = 11$ and 14, respectively) were subjected to direct staining for CD4, CD45RA, and FOXP3. (*C* and *D*) Representative plots of CCR7 and CD45RA expression by CD8^{+} T cells (*C*) and summary of each CD8^{+} T cell subsets (*D*). (*E*) CTLA-4–expressing clusters (dotted line) in PBMCs and TILs from melanoma patients by CyTOF analysis. viSNE plots of CD4^{+} and CD8^{+} T cells with heat maps for indicated marker expression levels are shown ($n = 2$). (*F*) Surface only or surface and intracellular staining of CTLA-4 in HD PBMC. (*G*) Surface CTLA-4 expressions by each cellular fraction from TILs and PBMCs of melanoma patients. Means ± SEM. *$P \leq 0.05$, **$P \leq 0.01$, ***$P \leq 0.001$, and ****$P \leq 0.0001$ by one-way ANOVA with post hoc Tukey's HSD test.

is instrumental in evoking and augmenting antitumor immune responses, as demonstrated recently with some monoclonal antibodies (mAbs) specific for the molecules specifically expressed by eTreg cells (13).

CTLA-4 is expressed by conventional T cells upon activation and by $FOXP3^+CD25^+CD4^+$ Treg cells constitutively. It plays a key role in Treg-mediated suppression, at least in part, via controlling CD80/CD86 expression by antigen-presenting cells (APCs) (14–16). Anti-human CTLA-4 mAb, which has been shown to be clinically effective in treating melanoma (17, 18), was initially considered to block CTLA-4–mediated negative signal into activated effector T cells, sustaining their activated state in attacking tumor cells. However, recent preclinical studies have shown that anti–CTLA-4 mAb is able to deplete $FOXP3^+$ Treg cells especially in tumor tissues, thereby augmenting tumor immunity (19–21). In humans, however, it is controversial whether CTLA-4 mAb affects the number or the function of Treg cells or effector T cells, or both, in enhancing antitumor immune responses in clinical contexts.

In this study, we have investigated in vivo and in vitro, in humans and mice, the effects of Fc-engineered anti–CTLA-4 mAbs on $FOXP3^+$ Treg cells and self/tumor antigen-specific $CD8^+$ T cells. We show that cell-depleting anti–CTLA-4 mAb with high antibody-dependent cell-mediated cytotoxicity (ADCC) activity is able to evoke antitumor immune responses depending on the levels and the kinetics of CTLA-4 expression by the two populations. The results can be extended to cell-depleting mAbs targeting other cell surface molecules that both Treg and effector T (Teff) cells commonly express at different levels and with different kinetics.

Results

Accumulation of CTLA-4–Expressing, Terminally Differentiated $FOXP3^{hi}$ eTreg Cells in Melanoma Tissues. We first assessed the frequency of various T cell subpopulations among tumor-infiltrating lymphocytes (TILs) in melanoma patients. $CD45RA^-FOXP3^{hi}$ eTreg cells (Fr. II) were predominantly (~10-fold) increased in ratio among $CD4^+$ TILs, compared with peripheral blood $CD4^+$ T cells in healthy donors or melanoma patients (Fig. 1 *A* and *B*). The frequency of $CD45RA^-FOXP3^{lo}$ Fr. III non-Treg cells also increased slightly (~twofold) among $CD4^+$ TILs. In contrast, $CD45RA^+FOXP3^{lo}$ naïve Treg cells (Fr. I) were significantly reduced in TILs to a quarter, on average, of the corresponding fraction in peripheral blood mononuclear cells (PBMCs). Among $FOXP3^-$ conventional $CD4^+$ T cells in TILs, $CD45RA^-FOXP3^-$ effector/memory $CD4^+$ T cells, which could be further dissected into the $CD25^+$ (Fr. IV) and the $CD25^-$ (Fr. V) populations (10), slightly (~1.3-fold) increased, while $CD45RA^+FOXP3^-$ naïve $CD4^+$ T cells (Fr. VI) significantly reduced to one-tenth of those in PBMCs. In the $CD8^+$ T-cell fraction of TILs, compared with PBMCs of the patients or healthy donors, there was a significant increase (~1.6-fold) of $CD45RA^-CCR7^-$ effector memory T (T_{EM}) cells, with significant decrease in $CD45RA^+CCR7^+$ naïve and $CD45RA^+CCR7^-$ terminally differentiated effector memory (T_{EMRA}) cells to a half and one-fifth, respectively, of those in PBMCs, and no significant change in $CD45RA^-CCR7^+$ central memory T (T_{CM}) cells (Fig. 1 *C* and *D*). It was also noted in melanoma patients that naïve $CD8^+$ T cells in PBMCs markedly (~14-fold) decreased compared with healthy donors.

We then assessed which T-cell population expressed CTLA-4 in TILs or PBMCs of melanoma patients by cytometry by time-of-flight (CyTOF) mass spectrometry cytometer (Fig. 1*E* and *SI Appendix*, Fig. S1*A*). The $CD4^+$ $CD45RA^-$ $Foxp3^{hi}$ cluster of cells, representing Fr. II eTreg cells, predominantly expressed CTLA-4 in PBMC and TIL, while $CD8^+$ T cells scarcely expressed CTLA-4 in either PBMC or TILs. In mice, predominant CTLA-4 expression by $FOXP3^+$ Treg cells was similarly observed in the spleen and CMS5a tumor tissue (*SI Appendix*, Fig. S1*B*). CTLA-4 expressed by human Fr. II eTreg cells was mostly in the intracellular compartment and cell-surface CTLA-4 was limited (Fig. 1*F*). Nevertheless, in TILs, eTreg cells, and to a lesser extent Fr. III non-Treg cells, were found to express surface CTLA-4 at significantly high levels (Fig. 1*G* and *SI Appendix*, Fig. S2). TIL $CD8^+$ T_{CM} and T_{EM} cells also expressed higher level of surface CTLA-4 compared with any of the circulating T cell fractions, although eTreg cells showed much higher expression in melanoma patients (Fig. 1*G* and *SI Appendix*, Fig. S2).

Taken together, cardinal features of human melanoma tissues are a marked increase and decrease of eTreg cells and naïve Treg cells, respectively, and a marked increase of effector/memory $CD8^+$ T cells with reduction of naïve $CD8^+$ T cells. These eTreg cells and $CD8^+$ T cells in TILs express CTLA-4 on the cell surface, with higher expression by the former than the latter. In contrast to TIL eTreg cells, circulating eTreg cells in melanoma patients are significantly lower in the level of surface CTLA-4 expression, suggesting that they may be less affected by anti–CTLA-4 mAb treatment.

Reduction of both eTreg Cells and Antigen-Specific $CD8^+$ T Cells by in Vitro Treatment with Cell-Depleting Anti–CTLA-4 mAb and Concurrent Antigen Stimulation. To address whether the antitumor effects of anti–CTLA-4 mAb would rely on its ability to deplete Treg cells by ADCC, we modified the Fc portion of anti–CTLA-4 IgG1 mAb (clone MDX-010, ipilimumab), which possessed a moderate ADCC activity, to change its affinity for FcγRIIIa (CD16a), an activatory FcγR expressed by NK cells, monocytes/macrophages, and other cells (22) (Fig. 2*A*). An anti–CTLA-4 mAb thus generated with a high ADCC activity, which we called asymmetric reengineering technology-Fc domain (ART-Fc), possessed different amino acid substitution on each heavy chain (23); that is, L234Y/L235Q/G236W/S239M/H268D/D270E/S298A substitutions into one heavy-chain Fc region and D270E/K326D/A330M/K334E substitutions into the other. The reconstructed mAb showed 1,000-fold higher binding affinity for human FcγRIIIa than unmodified mAb without increasing the affinity for inhibitory FcγRIIb. We also generated an anti–CTLA-4 mAb scarcely binding to FcγRs, which we called silent-Fc anti–CTLA-4, by amino acid substitutions; that is, L235R, G236R, and S239K into the Fc region of both heavy chains. Compared with unmodified or silent-Fc anti–CTLA-4 mAb, ART-Fc showed much higher in vitro cytotoxicity to CTLA-4–expressing Chinese hamster ovary (CHO) cells in the presence of PBMCs from healthy donors, with increased cytotoxicity by longer incubation (Fig. 2*B*). Similarly, ART-Fc anti–CTLA-4 mAb effectively killed freshly prepared Fr. II eTreg cells and, to a lesser extent, Fr. III non-Treg or Fr. I naïve Treg cells, while IgG1 (ipilimumab) or silent-Fc mAb scarcely showed killing activity (Fig. 2*C*).

Next, we assessed the effects of these Fc-engineered mAbs on in vitro antigen-specific expansion of $CD8^+$ T cells by stimulating PBMCs from HLA-A*0201–expressing healthy donors or melanoma patients for 9 d with various peptides, for example: derived from Melan-A/MART-1, a self/tumor-antigen expressed by normal melanocytes and some melanoma cells (24); and NY-ESO-1, a cancer/testis antigen expressed by various types of cancer cells and human germline cells (25), cytomegalovirus (CMV), or influenza (Flu) virus. This in vitro peptide stimulation, for example by Melan-A peptide, maintained the high expression of CTLA-4 by eTreg cells (Fig. 2*D* and *SI Appendix*, Fig. S3). The peptide stimulation alone also expanded peptide-specific tetramer $(Tet)^+$ $CD8^+$ T cells, which expressed higher levels of CTLA-4 especially on the cell surface, compared with Tet^- cells (Fig. 2 *E*, *F*, and *I*). When ART-Fc anti–CTLA-4 mAb was present from the beginning of the peptide stimulation of PBMCs from healthy donors or melanoma patients, the ratio of CTLA-4–expressing eTreg cells among $CD4^+$ T cells was significantly reduced in a dose dependent manner, while silent-Fc mAb failed to show this effect (Fig. 2 *D* and *G* and *SI Appendix*, Figs. S4 and S5).

The Treg cell reduction, however, did not accompany the expansion of antigen-specific $CD8^+$ T cells; rather, the treatment

IMMUNOLOGY AND INFLAMMATION

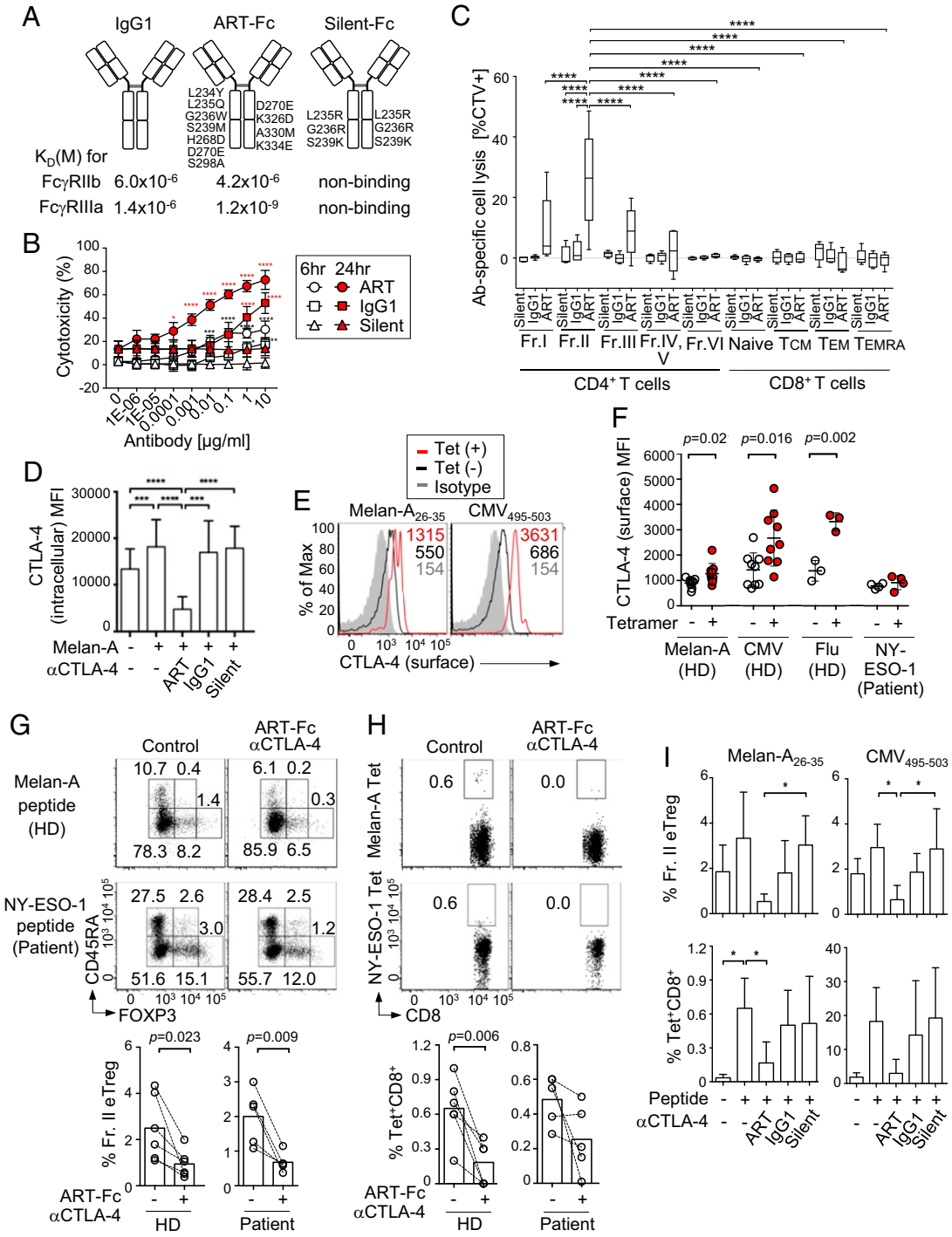

Fig. 2. Concurrent in vitro peptide stimulation with ART-Fc anti–CTLA-4 mAb restricts antigen-specific CD8$^+$ T cell responses. (*A*) Summary of amino acid substitutions made to the Fc portion of anti-human CTLA-4 IgG1 mAb (clone MDX-010, ipilimumab) to generate ART-Fc or silent-Fc mAbs, and their affinities to inhibitory FcγRIIb or activatory FcγRIIIa. Silent-Fc mAb affinity was below the detection limit of BIACORE assay. (*B*) ADCC activity of various anti–CTLA-4 mAbs against human CTLA-4–expressing CHO cells. Anti–CTLA-4 mAbs (ART, ADCC-enhanced anti–CTLA-4 ART-Fc; IgG1, conventional unmodified anti–CTLA-4 IgG1; Silent, Fc-region-inactivated anti-CTLA-4 silent-Fc) were incubated with CHO cells and HD PBMCs (n = 3) at an E/T ratio of 50:1. Means ± SEM. Asterisks indicate significant differences between each antibody and silent-Fc at respective concentrations for 6-h (black) or 24-h (red) cultures. (*C*) ADCC activity to each cellular fraction of CD4$^+$ and CD8$^+$ T cells from PBMCs by ART-Fc, IgG1, or silent-Fc anti–CTLA-4 mAbs (n = 4 or 5). Frequencies of dead cells among CTV prelabeled cells after 24-h culture are indicated. (*D*) CTLA-4 expression by Fr. II eTreg cells after 9 d of Melan-A peptide stimulation and 1 μg/mL ART-Fc, silent-Fc, or IgG1 anti-CTLA-4 mAb treatment to whole PBMCs (n = 7). (*E* and *F*) Surface CTLA-4 expressions by Tet$^+$ and Tet$^-$ CD8$^+$ T cells after indicated peptide stimulations. Representative histograms (*E*) and summary of mean flouorescence intensity (MFI) (*F*) (Melan-A, n = 9; CMV, n = 9; Flu, n = 3; ESO-1, n = 4). (*G* and *H*) Representative plots and frequencies of Fr. II eTreg cells (*G*) and antigen-specific CD8$^+$ T cells (*H*) from HDs (n = 6) or melanoma patients (n = 5) after the culture with indicated peptide and 1 μg/mL ART-Fc anti–CTLA-4 mAb as in *D*. (*I*) Quantification of the frequency of eTreg cells (*Upper*) and Tet$^+$ CD8$^+$ T cells (*Lower*) after 9 d of Melan-A or CMV antigen stimulation to HD PBMCs with indicated anti-CTLA-4 mAbs in *G* and *H*. Means ± SEM. Depicted significance between two groups were calculated using paired *t* test, one-way ANOVA, or two-way ANOVA with post hoc Tukey's HSD test. *$P \leq 0.05$, **$P \leq 0.01$, ***$P \leq 0.001$, and ****$P \leq 0.0001$.

caused a profound reduction of the ratio of Tet$^+$ CD8$^+$ T cells among CD8$^+$ T cells (Fig. 2*H*). In these in vitro stimulations, unmodified IgG1 or silent-Fc anti–CTLA-4 mAb did not exhibit significant eTreg-depleting activity (Fig. 2*I*). The degree of eTreg cell reduction by these mAbs was indeed correlated with the reduction of antigen-specific CD8$^+$ T cells, regardless of the stimulating antigen, for example, Melan-A or CMV peptide (Fig. 2*I*).

Thus, while eTreg cells constitutively express CTLA-4, especially intracellular CTLA-4, antigen-stimulation expands CD8$^+$ T cells that express high levels of CTLA-4, particularly on the cell surface. ART-Fc anti–CTLA-4 mAb with high ADCC activity is therefore able to deplete not only CTLA-4$^+$ eTreg cells but also antigen-activated CTLA-4$^+$ CD8$^+$ T cells. This effector CD8$^+$ T-cell depletion may offset an immune-enhancing effect of eTreg cell depletion in immune responses in vitro.

Robust Expansion of Antigen-Specific CD8$^+$ T Cells by eTreg Cell Depletion Before Antigen Stimulation. We next attempted to deplete CTLA-4$^+$ Treg cells before antigen stimulation to spare antigen-activated CTLA-4–expressing CD8$^+$ T cells from killing by anti–CTLA-4 mAbs. We cultured whole PBMCs from healthy donors or melanoma patients in the presence of ART-Fc anti–CTLA-4 mAb for 5 d without antigen stimulation, removed the mAb, then stimulated the cells with various peptides for 8 d, and analyzed them for the ratio of eTreg cells and Tet$^+$ CD8$^+$ T cells among CD4$^+$ T cells or CD8$^+$ T cells, respectively (Fig. 3*A*). The ratio of FOXP3^{hi} eTreg cells was significantly reduced within 5 d by the ART-Fc pretreatment (Fig. 3*A* and *SI Appendix*, Fig. S6), and maintained at a low level during subsequent peptide stimulation (Fig. 3*B*), indicating that eTreg cells had not fully recovered during the antigen-stimulation period. This ART-Fc pretreatment combined with antigen stimulation induced robust expansion of Melan-A–specific CD8$^+$ T cells from healthy donor PBMCs, and NY-ESO-1–specific CD8$^+$ T cells from PBMCs of patients whose melanoma tissues expressed NY-ESO-1 (Fig. 3*C*). CMV-specific CD8$^+$ T cells were not much affected by ART-Fc–mediated Treg depletion. In contrast with ART-Fc, silent-Fc anti–CTLA-4 mAb did not alter the frequency of eTreg cells, and failed to expand Tet$^+$ CD8$^+$ T cells regardless of antigen species (Fig. 3*D*).

One of various suppression mechanisms used by Treg cells is CTLA-4–dependent down-regulation of CD80 and CD86 expression by dendritic cells (DCs) (14, 15). To investigate possible contributions of this mechanism to the expansion of self/tumor antigen-specific CD8$^+$ T cells after in vitro ART-Fc anti–CTLA-4 mAb treatment, we assessed CD80 and CD86 expression by DCs, which were phenotypically defined as Lin-1$^-$CD11c$^+$HLA-DR$^+$, in healthy donor PBMCs. Both CD80 and CD86 expression showed distinct up-regulation in the ART-Fc pretreated group, in contrast to unaltered CD80/CD86 expression in an unmodified IgG1-pretreated, silent-Fc–pretreated, or untreated group (Fig. 3*E*). In addition, the degree of FcγR-binding affinities of mAbs had a good correlation with their Treg depletion activity and also with Tet$^+$ CD8$^+$ T cell-inducing activity (Fig. 3*F*). Because mere blockade of CTLA-4 by silent-Fc did not up-regulate CD80/86, the results indicated that eTreg depletion by ART-Fc activated DCs, although a possibility exists that ART-Fc itself might additionally contribute to the activation of DCs via high affinity binding to their activatory Fc receptors.

Taken together, these results indicate that Treg depletion by ART-Fc anti–CTLA-4 mAb several days before antigen exposure is able to spare the killing of CTLA-4$^+$ antigen-activated CD8$^+$ T cells by the antibody, expanding them, at least in part, via enhancing CD80/CD86 expression by APCs.

CTLA-4–Mediated Treg-Depletion Before Tumor Antigen Vaccination Enhances Antitumor Responses in Mice. To validate in mice the in vitro findings with human PBMCs and anti-human CTLA-4 mAbs, we generated mAbs with a high or low ADCC and antibody-dependent cellular phagocytosis (ADCP) activity from anti-mouse CTLA-4 mAb (clone UC10) of IgG2a isotype (called mIgG2a hereafter) by amino acid substitution in the Fc domain (Fig. 4*A*). The mutation S239D in both heavy chains raised the affinity for mouse FcγRIV ∼sevenfold (mFa55 mIgG2a variant), while L235R, G236R, and S239K mutations in both heavy chains rendered them nonbinding to mouse FcγRs (mFa31 mIgG2a variant); the former was called mouse ADCC/ADCP–enhanced-Fc (mEnhanced), the latter mouse silent-Fc (mSilent) mAb. To compare antitumor activity of these Fc-modified anti-mouse–CTLA-4 mAbs in combination with tumor antigen vaccination, we subcutaneously inoculated into BALB/c mice CMS5a fibrosarcoma cells expressing human NY-ESO-1 antigen, and on day 9, when the tumor became established, treated the mice with 100 μg of each mAb and vaccinated with NY-ESO-1 peptide on the same day (day 9; we hereafter call the protocol "concurrent treatment") or 3 d later (day 12; hereafter "Ab pre-treatment") (Fig. 4*B*). Ab pretreatment with mEnhanced mAb was more effective than concurrent treatment or pretreatment with either mIgG2a or mSilent mAb in retardation of tumor growth; the effects of the latter two mAbs on tumor growth were low and not significantly different between Ab pretreatment and concurrent treatment (Fig. 4*C*). The survival was significantly better in mice pretreated with mEnhanced mAb, and also in mice with concurrent treatment or pretreatment with mIgG2a, although either way of mIgG2a treatment failed to induce tumor regression in most of the mice (Fig. 4 *C* and *D*).

The mEnhanced mAb pretreatment also resulted in a significant increase in the number of tumor-infiltrating CD8$^+$ T cells and the CD8/Treg ratio in TILs, albeit the percentage of FOXP3$^+$ cells among CD4$^+$ T cells slightly increased (Fig. 5 *A*–*C*). In addition, whereas the frequency of NY-ESO-1 peptide-specific CD8$^+$ TILs was not statistically different among the mice treated with each mAb or between pretreatment and concurrent treatment, the antigen-specific CD8$^+$ TILs from mEnhanced mAb pretreated mice, compared with other groups, showed significantly more active IL-2 and IFN-γ production upon in vitro restimulation with NY-ESO-1 peptide (Fig. 5 *D* and *E*). Moreover, effector memory CD8$^+$ T cells defined as the CD44^{high}CD62L^{low} population significantly increased among NY-ESO-1–specific CD8$^+$ TILs in mEnhanced mAb pretreated mice (Fig. 5 *F* and *G*).

Taken together, mEnhanced mAb pretreatment was most effective in evoking tumor immunity, followed by pretreatment with mIgG2a, which had some ADCC activity, while mSilent mAb was much less effective. The results indicate that pretreatment of tumor-bearing mice with ADCC/ADCP-enhanced anti–CTLA-4 mAb followed by tumor antigen vaccination is able to effectively evoke antitumor immune responses in vivo.

Discussion

The major findings in this report are: (*i*) terminally differentiated, highly suppressive eTreg cells are abundant in tumor tissues and expressing surface CTLA-4 at higher levels than tumor-infiltrating CD8$^+$ T cells; (*ii*) anti–CTLA-4 mAb with high ADCC activity is capable of depleting/reducing CTLA-4^{high} eTreg cells and CTLA-4$^+$ effector CD8$^+$ T cells; and (*iii*) cell-depleting anti–CTLA-4 mAb is able to evoke and enhance effective tumor immunity when the antibody treatment regimen is devised not to affect CTLA-4$^+$ effector CD8$^+$ T cells, for example, by altering the timing of Treg cell depletion and cancer antigen vaccination.

The ADCC activity of anti–CTLA-4 mAb is a key determinant of the effectiveness of eTreg reduction and resulting expansion of tumor-reactive CD8$^+$ T cells. Supporting the notion, we demonstrated that anti–CTLA-4 mAb (ART-Fc) with an enhanced ADCC activity (and/or ADCP activity in mice) was able to augment antitumor immune responses in vitro in humans and in vivo in mice by depleting CTLA-4–expressing Treg cells. Anti–CTLA-4 mAbs (silent-Fc) modified to exhibit a much less or no ADCC activity failed to show such antitumor activity, even if they possessed

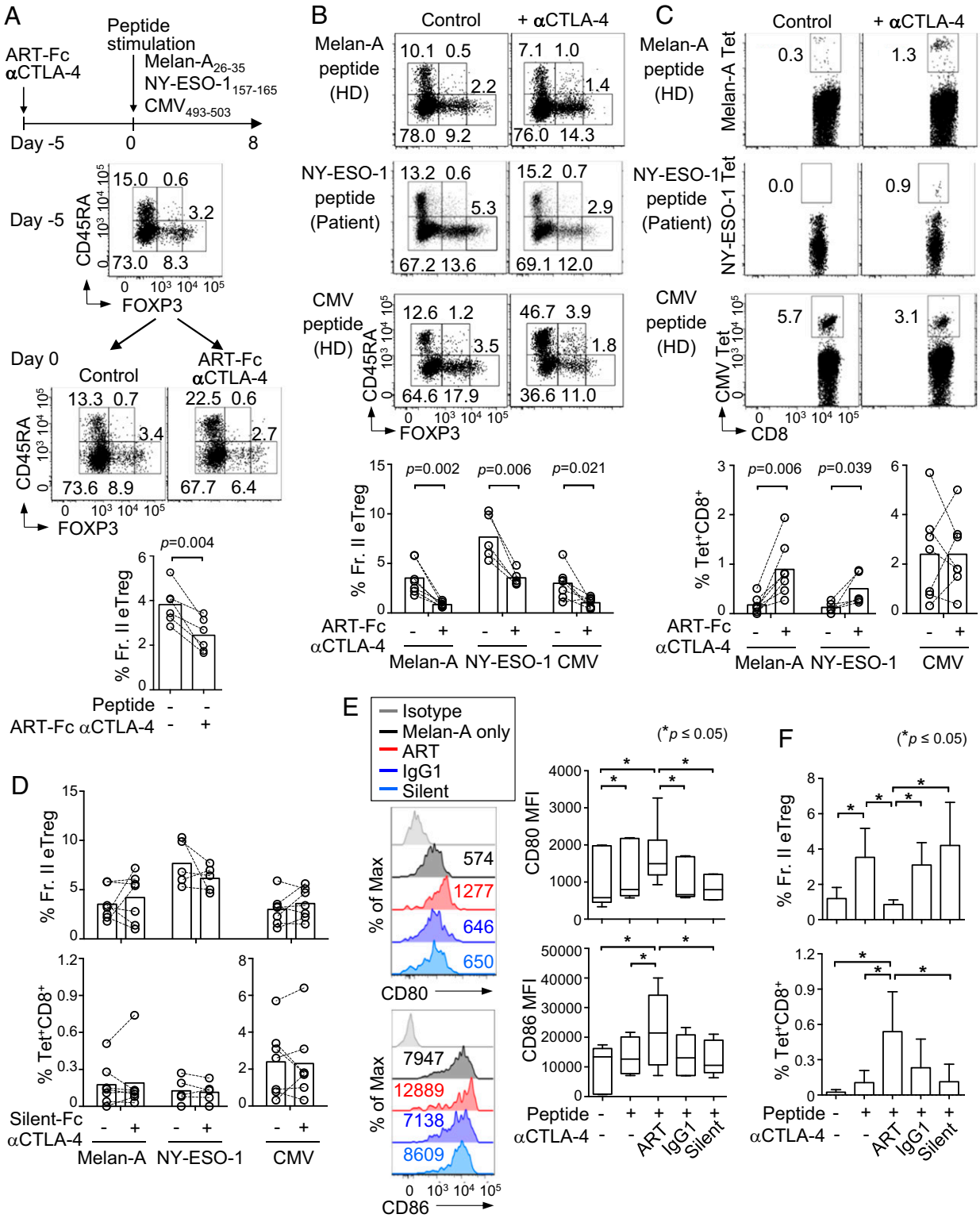

Fig. 3. Predepletion of Treg cells using ART-Fc anti–CTLA-4 mAb enhances self/tumor antigen-specific CD8$^+$ T cell responses. (*A–D*) Antigen-specific CD8$^+$ T cell were induced from whole PBMCs of HDs (n = 7) or patients (*n* = 5) after 5 d of pretreatment with ART-Fc anti–CTLA-4 mAb. (*A*) Scheme of the experiment and representative FOXP3 and CD45RA staining of CD4$^+$ T cells at day −5 and day 0 of the experiment. Summary of Fr. II eTreg frequencies at day 0 (*Bottom*). (*B* and *C*) Representative FOXP3 staining of CD4$^+$ T cells (*B*) and antigen-specific CD8$^+$ T cells (*C*) with or without ART-Fc pretreatment for each peptide after the culture. Summary of eTreg and antigen-specific CD8$^+$ T cell frequencies after the culture (*Bottom*). (*D*) Summary of Fr. II eTreg and Tet$^+$ CD8$^+$ T cell frequencies with silent-Fc anti–CTLA-4 mAb pretreatment instead of ART-Fc as in *A–C*. (*E*) Expression levels of CD80 and CD86 by Lin-1$^-$CD11c$^+$HLA-DR$^+$ DCs after 5 d of Melan-A stimulation with the pretreatment of indicated anti–CTLA-4 mAbs (*n* = 6). Numbers on histograms show MFI. (*F*) Summary of eTreg and Tet$^+$CD8$^+$ T cell frequencies after pretreatment with indicated anti–CTLA-4 mAbs followed by Melan-A$_{26–35}$ stimulation as in *A–C*. Means ± SEM. Depicted significance between two groups were calculated using paired *t* test. *$P \leq 0.05$.

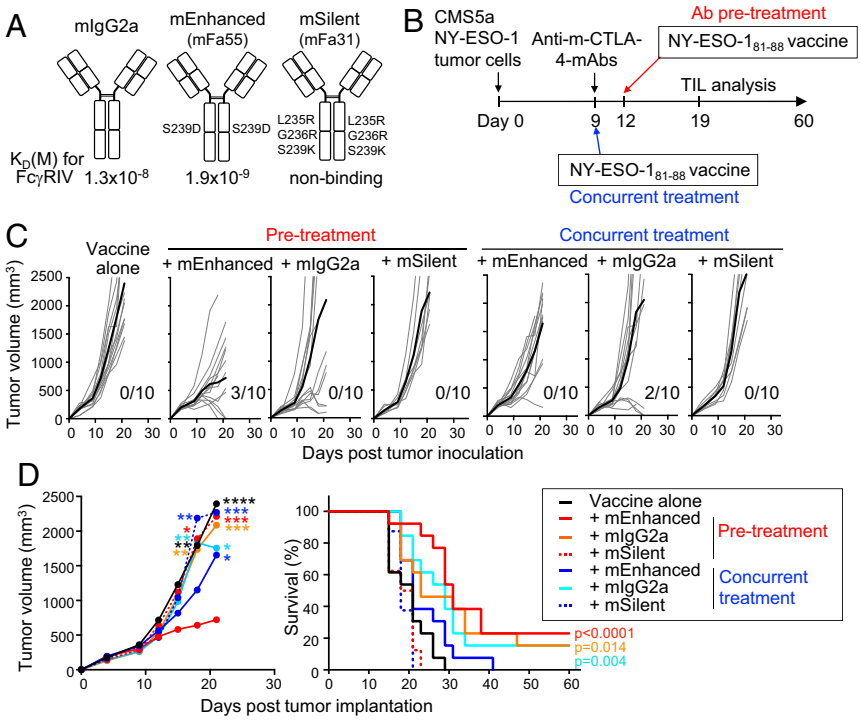

Fig. 4. Pretreatment with ADCC/ADCP-enhanced anti–CTLA-4 mAb induces strong antitumor effects in mice. (*A*) Summary of amino acid substitutions made to the Fc portion of anti-mouse CTLA-4 IgG2a mAb (clone UC10; mIgG2a) to generate ADCC/ADCP-enhanced anti-mouse–CTLA-4 (mEnhanced) or silent-Fc anti-mouse–CTLA-4 (mSilent) mAbs, and their affinities to mouse FcγRIV are shown. mSilent mAb affinity was below the detection limit of BIACORE assay. (*B*–*D*) Scheme of the experiment (*B*). Mice were challenged with 2×10^6 CMS5a fibrosarcoma expressing human NY-ESO-1 on day 0, and left untreated or treated with mEnhanced, mIgG2a, or mSilent anti-mouse–CTLA-4 mAb on day 9. Vaccination of NY-ESO-1$_{81-88}$ peptides mixed with CFA was performed on the same day (day 9, concurrent treatment) or 3 d later (day 12, Ab pretreatment). Tumor growth of each mice with bold line indicating the average of each treatment group (*C*) (n = 8–13 per group). Summary of average tumor growth of each treatment groups (*D*, *Left*). Asterisks indicate P values between mEnhanced mAb pretreatment group by two-way ANOVA with Tukey's multiple comparison test. Summary of survival rate (*D*, *Right*) of each treatment groups. P values between the survival of each groups and the survival of vaccine-alone control were calculated by log-rank test. Death event corresponds to tumor length over ≥200 mm or death of the mouse. *$P \leq 0.05$, **$P \leq 0.01$, ***$P \leq 0.001$, and ****$P \leq 0.0001$.

the same specificity for an epitope of the CTLA-4 molecule. It remains unclear in humans whether the antitumor effect of ipilimumab with IgG1 Fc portion is attributed to blockade of the CTLA-4 molecule or depletion of CTLA-4–expressing cells by ADCC. It was shown in mice that an enhancement of antitumor immunity by an anti–CTLA-4 mAb required depletion of tumor-infiltrating Treg cells by FcγR-mediated ADCC (19–21, 26, 27). Similarly, antibodies against GITR, OX40, and CD25 molecules, which tumor-infiltrating Treg cells express the highest amounts, were shown to be dependent on ADCC-mediated depletion of Treg cells in tumor rejection (19, 26, 28). It was also reported that ipilimumab treatment of melanoma patients significantly reduced FOXP3$^+$ Treg cells in the tumor tissues particularly in clinical responders (29). In addition, a recent report has shown that, among melanoma patients with high tumor mutation burden, those genetically having a high-affinity variant of FcγRIIIa with enhanced ADCC (V158 variant, as opposed to the F158 low-affinity variant) showed significantly better clinical responses to ipilimumab treatment and better overall survival (27). This finding supports the notion that anti–CTLA-4 mAb with better Treg depletion activity may be more effective than ipilimumab in cancer immunotherapy. It is thus likely that ART-Fc anti–CTLA-4 mAb, which possesses a high affinity for V158 variant ($K_D = 3.7 \times 10^{-10}$ M, compared with 3.1×10^{-6} M for ipilimumab or IgG1), may have a better clinical efficacy in cancer immunotherapy via depleting Treg cells. Taken together, these findings in humans and mice indicate that high-ADCC/ADCP anti–CTLA-4 mAb can be effective in evoking and enhancing tumor immunity via depleting Treg cells.

A key feature of CTLA-4 expression is that it is mostly located in intracellular vesicles (~90%) and T cell receptor stimulation promotes trafficking of CTLA-4 to the cell surface (30–32). Our CyTOF analysis showed that eTreg cells in the PBMCs and melanoma tissues are the predominant cluster of cells expressing high amounts of CTLA-4 in total: that is, intracellular and surface CTLA-4. The quantity of CTLA-4 expression on the cell surface was also highest by TIL eTreg cells; and TIL CD8$^+$ T_{CM} and T_{EM} expressed higher levels compared with any of the circulating T cell populations—including eTreg cells—in the PBMC. Given their highly activated state of tumor-infiltrating eTreg and CD8$^+$ T cells (e.g., CD69^{high} by CyTOF analysis) (*SI Appendix*, Fig. S1*A*), these cells apparently increased the amount and ratio of CTLA-4 retained at the cell surface upon stimulation. Although the precise mechanism regulating cell surface expression of CTLA-4 by its cytoplasmic tail is not fully understood, the quantity of cell surface CTLA-4 and the kinetics of its expression are key determinants of the efficacy in killing CTLA-4–expressing cells by high-ADCC anti–CTLA-4 mAb.

Treg cells and CD8$^+$ CTLs are different at the levels and in the kinetics of CTLA-4 expression. High-ADCC anti–CTLA-4 mAb can therefore achieve predominant depletion of Treg cells without much affecting CD8$^+$ T cells when the level of cell surface CTLA-4 expressed on Treg cells is higher than that of CD8$^+$ T cells. Indeed, in human melanoma tissues, surface CTLA-4 expression was highest on Fr. II eTreg cells, followed by Fr. III non-Treg cells, T_{EM} CD8$^+$, and T_{CM} CD8$^+$ T cells. However, antigen stimulation expands antigen-specific CD8$^+$ T cells expressing CTLA-4, rendering them a target of anti–CTLA-4 mAb. This was evident in our simultaneous treatment of ART-Fc anti–CTLA-4 mAb and peptide stimulation, which

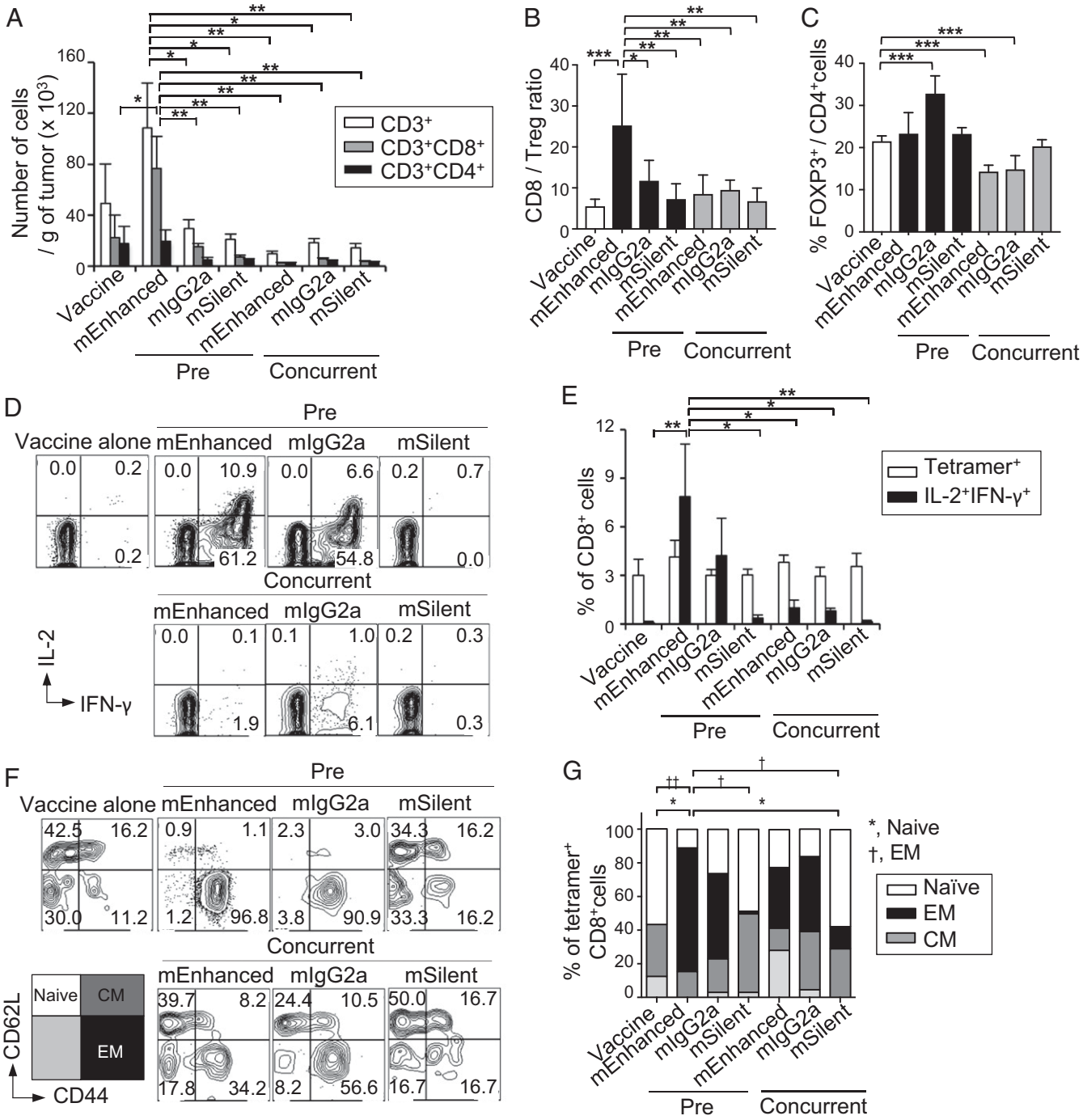

Fig. 5. Ag-specific CD8$^+$T cell responses induced in tumor-bearing mice by pretreatment with ADCC/ADCP-enhanced anti–CTLA-4 mAb. (*A*–*G*) TILs from Fig. 4 were analyzed 19 d after tumor implantation (n = 4–6 per group). The number of infiltrated T cells per gram of tumor (*A*). CD8/Treg cell ratio (*B*). Frequency of Foxp3$^+$Treg cells among CD4$^+$ T cells (*C*). Representative plots of IL-2$^+$ IFN-γ$^+$ CD8$^+$ T cells (*D*). Cytokine production was measured by restimulating TILs with ESO-$1_{81–88}$ peptides in vitro for 5 h. Summary of Tet$^+$ CD8$^+$ T cells in the tumor, and IL-2$^+$ IFN-γ$^+$ CD8$^+$ T cells in *D* after the restimulation (*E*). Representative plots (*F*) and summary (*G*) of CD44 and CD62L expressions by NY-ESO-1-Tet$^+$ CD8$^+$ T cells in the tumor of each treatment groups. Data were obtained from three independent experiments. *P* values between Naïve or EM CD8$^+$ T cell subsets of each conditions. Means ± SEM. $^*P \leq 0.05$, $^\dagger P \leq 0.05$, $^{**}P \leq 0.01$, $^{\dagger\dagger}P \leq 0.01$, and $^{***}P \leq 0.001$ by two-way ANOVA with Tukey's multiple comparison test.

reduced both eTreg and antigen-specific CD8$^+$ T cells. One way to circumvent this inconvenience is to combine high-ADCC anti–CTLA-4 mAb treatment with delayed antigenic stimulation because Treg cells, especially human eTreg cells, are constitutively expressing CTLA-4 but CD8$^+$ T cells express the molecule only after antigenic stimulation. Indeed, 3-d delay in peptide vaccination in mice, or 5-d delay in peptide stimulation in human PBMC culture, following ART-Fc anti–CTLA-4 mAb treatment was effective in sparing antigen-specific CD8$^+$ T cells from ADCC killing, and augmented antitumor immunity. Similar findings were also made with anti-CD25 IgG2a mAb (clone PC61) in mice: tumor regression by pretreatment with the mAb 4 d before tumor cell

inoculation while no tumor regression by the mAb treatment on the same day or after the tumor inoculation (33). In agreement with these results, simultaneous treatment of ipilimumab and gp100 peptide vaccine in patients with metastatic melanoma showed slight reductions in overall survival compared with ipilimumab alone, suggesting that melanoma-antigen specific $CD8^+$ T cells with elevated CTLA-4 expression might have been concurrently targeted and reduced by ipilimumab in these patients (17, 34). Furthermore, because the presence of ART-Fc was required for only a few days before vaccination to enhance tumor immunity, the duration and the amount of ipilimumab could be reduced in cancer immunotherapy to lessen its immune-related adverse events. Collectively, these results demonstrate critical importance of designing an immunologically rational sequence of treatments: that is, Treg depletion before tumor-antigen stimulation.

In conclusion, because CTLA-4–expressing terminally differentiated eTreg cells abundantly infiltrate into a variety of tumors, it is necessary to first reduce them from the tumor environment to make the current cancer immunotherapy (such as activation of effector T cells by immune checkpoint blockade or cancer antigen vaccination) more effective. Our results not only highlight the therapeutic potential of cell-depleting anti–CTLA-4 mAb for Treg cell depletion but also help designing cancer immunotherapy with other cell-depleting mAbs targeting other molecules, such as CD25, GITR, and OX40, which can be commonly expressed, but at different expression levels or with different kinetics, by both Treg and effector T cells.

Materials and Methods

Donor Samples. Peripheral blood samples were obtained from healthy individuals or patients with stage III to IV melanoma. PBMCs were isolated by density gradient with Ficoll-Paque (GE Healthcare). TILs were obtained from resected melanoma tissues. Tumor was minced, and single-cell suspensions generated after gentleMACS dissociation (Miltenyi) were prepared by filtering through a 40-μm cell strainer. All donors provided written informed consent before sampling according to the Declaration of Helsinki. The present study was approved by the Institutional Review Board of Osaka University.

CyTOF Analysis. TILs and splenocytes from tumor-bearing mice were enriched for $CD3^+$ cells and stained with 198-cisplatin for dead cell discrimination and a panel of antibodies including the following metal-conjugated antibodies: 172Yb-CD4 (RM4-5), 168Er-CD8 (53-6.7), 164Dy-CTLA-4 (UC-10), 158Gd-FOXP3 (FJK-16s). For human PBMCs and TILs, cell suspensions were barcoded by anti-CD45 antibodies with various metal-conjugates, as described previously (35), before staining with 198-cisplatin for dead cell discrimination and then antibody staining with the following panel. Metal-conjugated antibodies were obtained from Fluidigm or Maxpar Antibody Labeling kit (Fluidigm) was used according to the manufacturer's instructions to conjugate purified antibodies: 89Y-CD45 (clone: HI30; Fluidigm), 115In-CD45 (HI30; Biolegend), 175Yb-CD45 (HI30; Biolegend) antibodies were used for barcoding different samples; CLA-FITC (HECA-452; BD), CCR8-PE (L263G8; Biolegend), CXCR5-Biotin (RF8B2; BD), eVolve 605 (114 Cd)-CD8a (RPA-T8; eBioscience), 139La-CD123 (6H6; Biolegend), 141Pr-CCR6 (11A9; Fluidigm), 142Nd-CD14 (M5E2; Biolegend), 144Nd-FITC (CLA) (FIT22; Fluidigm), 145Nd-CD4 (RPA-T4; Fluidigm), 148Sm-CD20 (2H7; Biolegend), 149Sm-CCR4 (205410; Fluidigm), 150Nd-SAV (CXCR5) (1D4-C5; Fluidigm), 151Eu-ICOS (C398.4A; Fluidigm), 152Sm-CD69 (FN50; Biolegend), 153Eu-CD45RA (HI100; Fluidigm), 154Sm-CD3 (UCHT1; Fluidigm), 155Gd-CD197 (CCR7) (150503; R&D Systems), 156Gd-anti-PE (CCR8) (PE001; Fluidigm), 158Gd-CD27 (L128; Fluidigm), 159Tb-CD19 (HIB19; Biolegend), 160Gd-CD39 (A1; Fluidigm), 163Dy-CXCR3 (G025H7; Fluidigm), 164Dy-CD95 (DX2; Fluidigm), 165Ho-CD45RO (UCHL1; Fluidigm), 166Er-CD279 (PD-1) (EH12.2H7; Biolegend), 167Er-PDL1 (29E.2A3; Biolegend), 169Tm-CD25 (IL-2R) (2A3; Fluidigm), 171Yb-CD11c (3.9; Biolegend), 172Yb-CD38 (HIT2; Fluidigm), 173Yb-TIGIT (MBSA43; eBioscience), 174Yb-HLA-DR (L243; Fluidigm), 176Yb-CD127 (IL-7R) (A019D5; Fluidigm), 209Bi-CD11b (ICRF44; Fluidigm), 146Nd-Helios (22F6; Biolegend), 161Dy–CTLA-4 (14D3; Fluidigm), 162Dy-FOXP3 (236A/E7; eBioscience), and 168Er-K_i-67 (K_i-67; Fluidigm). Human and mouse cells were fixed with eBioscience Foxp3/transcription factor staining buffers (ThermoFisher) before intracellular staining. Stained cells were then resuspended in 2% PFA with 191/193-iridium DNA intercalator (Fluidigm) overnight then washed and resuspended in Maxpar water (Fluidigm) and EQ four-element beads (Fluidigm) immediately before the analysis with Helios CyTOF system (Fluidigm). Normalized data were analyzed with Cytobank Premium (https://Cytobank.org).

Stimulation of Antigen-Specific $CD8^+$ T Cells. Whole PBMCs from healthy individuals and melanoma patients were stimulated with 10 μM of short peptides specific for HLA-A*0201 (Operon Biotechnology) for 8–9 d: Melan-$A_{26–35}$ (EAAGIGILTV), $CMV_{495–503}$ (NLVPMVATV), $Flu_{58–66}$ (GILGFVFTL), or NY-ESO-$1_{157–165}$ (SLLMWITQC) (12, 22). To determine the effect of anti–CTLA-4 mAb with various ADCC, one of the following mAbs was added to the culture at 1 μg/mL (unless otherwise indicated) on the same day or 5 d before antigen stimulation: ADCC-enhanced anti-human–CTLA-4 IgG1 (MDX-010-ART-Fc), conventional unmodified anti–CTLA-4 IgG1 (MDX-010-IgG1), or silent-Fc anti–CTLA-4 IgG1 antibodies (MDX-010-silent-Fc): All mAbs were kindly provided by Chugai Pharmaceutical. One-half of the medium was replaced with fresh medium containing 10 U/mL IL-2 and 40 ng/mL IL-7 every 3 d.

Lactate Dehydrogenase-Release Assay with Human CTLA-4–Expressing CHO Cells. Lactate dehydrogenase (LDH)-release assay was performed to determine the ADCC activity in PBMCs. The CHO DG44-hCTLA4 cells (from Chugai Pharmaceutical) were seeded onto 96-well round-bottom plates (1×10^4 cells per well), and incubated with various concentrations of mAbs for 15 min. PBMCs obtained from healthy donors were then added to the culture at an effector-to-target (E/T) ratio of 50:1. Cells were incubated at 37 °C, 5% CO_2 for 6 or 24 h, 100μL of the supernatant from each well was collected and absorbance of 492 nm and 630 nm was measured using Cytation 5 Cell Imaging Multi-Mode Reader (BioTek Instruments). LDH release was considered to be at maximum after incubation of the cells in 1% Nonidet P-40 solution. The cytotoxicity (%) was determined from the formula; $(A - C)(B - C) \times 100$, where A, B, and C represent LDH release of each experiment, maximum LDH release, and background LDH release, respectively. All experiments were performed in duplicate.

ADCC Assay with Freshly Isolated Human PBMC. PBMCs from healthy donors were FACS sorted for each fractions of T and Treg cells were prelabeled with CellTrace Violet (CTV; ThermoFisher), and cultured with non-T cells, as effector cells, at 1:50 target-to-effector ratio. Next, 1 μg/mL of indicated anti–CTLA-4 mAb was added to 10% human AB serum containing RPMI-1640 medium with 5 IU/mL IL-2. After 24-h culture at 37 °C, frequency of dead cells, indicated by LIVE/DEAD fixable staining (ThermoFisher), among CTV^+ cells were assessed by FACS.

Murine Tumor Experiments. Six- to 7-wk-old BALB/c mice were purchased from CLEA Japan, and maintained under specific pathogen-free conditions. Mice were subcutaneously challenged with 2×10^6 CMS5a-NY-ESO-1. Nine days after the tumor implantation, mice received 100 μg of anti-mouse–CTLA-4 mAb (UC-10 clone; mIgG2a, mEnhanced, or mSilent, from Chugai Pharmaceutical) intravenously. mEnhanced variant (mFa55 mIgG2a variant) was generated by S239D mutation in the CH2 domain, and shows improved binding affinity to mouse FcγRIV by approximately sevenfold compared with wild-type mIgG2a. Mice were treated with vaccination of 100 μg of ESO-$1_{81–88}$ peptides (Operon Biotechnology) mixed with 200 μL of CFA/PBS (1:1 ratio) either on the same day (day 9, concurrent treatment) or 3 d later (day 12, Ab pretreatment) subcutaneously. Tumor size was measured every 3–4 d. Experiments were approved by the Institutional Review Board and conducted in compliance with Osaka University regulations.

Flow Cytometry. As described previously (12, 23), in vitro generated antigen-specific $CD8^+$ T cells were stained with PE-labeled Melan-A, CMV, or Flu tetramer (TC Matrix) or PE-labeled NY-ESO-1 tetramer (MBL) for 10 min at 37 °C, and then stained with various surface mAbs. For the staining of surface CTLA-4 in this study, biotinylated–anti-human CD152 antibody (clone BNI3; BD Biosciences) was used at 4 °C for 15 min with other antibodies against surface molecules. After washing, we added APC-streptavidin (Biolegend) also at 4 °C for 15 min to avoid staining of CTLA-4 molecules externalized to the surface after extended staining condition at 37 °C. These staining procedures were performed before fixation and permeabilization, as described in our previous study (24). Intracellular staining of FOXP3 was performed using FOXP3 Transcription Factor Staining Buffer set (eBioscience). Following antibodies with indicated fluorescent labels were used for staining human cells: PerCP/Cy5.5-CCR7 (150503; BD Biosciences), FITC-CD45RA (HI100; BD Biosciences), biotin–CTLA-4 (BNI3; BD Biosciences), APC-Streptavidin (BioLegend), V500-CD8 (RPA-T8; BD Biosciences), BrilliantViolet711-CD3 (OKT3; Biolegned), AlexaFluor700-CD4 (RPA-T4; eBioscience), FITC-Lineage mixture (BD Biosciences), PerCP/Cy5.5-CD11c (3.9; BioLegend), APC-HLA-DR (LN3; eBioscience), PE-CD86

(IT2.2; eBioscience), AlexaFluor700-CD80 (L307.4; BD Biosciences), PE-FOXP3 (236A/E7; eBioscience), and fixable viability dye eFluor780 (eBioscience). Following antibodies were used to stain mouse cells: V500-CD8 (53-6.7; BD Biosciences), PE-Cy7-CD3e (145-2C11; eBioscience), eFluor450-CD4 (RM4-5; eBioscience), APC-CD25 (PC61.5; eBioscience), PE-FOXP3 (FJK-16s; eBioscience), FITC–IFN-γ (XMG1.2; BD Biosciences), AlexaFluor647-IL-2 (JES6-5H4; eBiosciences) and fixable viability dye eFluor780 (eBioscience). Antigen-specific TIL $CD8^+$ T cells from mice were stained with PE-labeled, H-$2D^d$-restricted ESO-$1_{81–88}$ tetramer (TC Matrix), as described above. To measure cytokine production from $CD8^+$ T cells, mouse TILs were restimulated for 5 h at 37 °C in the presence of 10 μM of the same ESO-$1_{81–88}$ peptides used for vaccination with GolgiPlug (BD Bioscience). Fixation and permeabilization were performed with the Cytofix/Cytoperm buffer set (BD Bioscience). Cells were acquired with LSR Fortessa (BD Bioscience), and analyzed using FlowJo v9.9.5 software.

Statistical Analysis. Two-tailed paired *t* test was used to evaluate significance between two groups. One-way or two-way ANOVA with post hoc Tukey's honest significant difference (HSD) test was used for comparing multiple groups. All statistical analyses were performed using Prism v6 software (Graphpad). P values < 0.05 were considered significant.

ACKNOWLEDGMENTS. We thank members of Department of Dermatology, Graduate School of Medicine, Osaka University for collecting patient samples; and K. Teshima, T. Shimizu, and N. Mizoguchi for technical assistance. Fc-engineered anti-human and mouse CTLA-4 antibodies were generated and provided by Chugai Pharmaceutical Co., Ltd. This study was supported by Grant-in-Aid for Specially Promoted Research 16H06295 (to S.S.), Grants-in-Aid for Scientific Research (A) 26253030 (to S.S.) and (B) 26290054 (to H.N.), Grant-in-Aid for challenging Exploratory Research 26670581 (to H.N.), and Grant-in-Aid for Young Scientists (B) 26860331 and 17K15723 (to A. Tanaka) from the Ministry of Education, Culture, Sports, Science and Technology of Japan; and Core Research for Evolutional Science and Technology from Japan Science and Technology Agency (S.S.). This study was partly performed as a research program of the Project for Development of Innovative Research on Cancer Therapeutics (P-DIRECT), and Practical Research for Innovative Cancer Control, and Project for Cancer Research and Therapeutic Evolution (P-CREATE) by the Japan Agency for Medical Research and Development.

1. Sakaguchi S (2004) Naturally arising CD4+ regulatory T cells for immunologic self-tolerance and negative control of immune responses. *Annu Rev Immunol* 22:531–562.
2. Zou W (2006) Regulatory T cells, tumour immunity and immunotherapy. *Nat Rev Immunol* 6:295–307.
3. Tanaka A, Sakaguchi S (2017) Regulatory T cells in cancer immunotherapy. *Cell Res* 27: 109–118.
4. Quezada SA, Peggs KS, Curran MA, Allison JP (2006) CTLA4 blockade and GM-CSF combination immunotherapy alters the intratumor balance of effector and regulatory T cells. *J Clin Invest* 116:1935–1945.
5. Shimizu J, Yamazaki S, Sakaguchi S (1999) Induction of tumor immunity by removing CD25+CD4+ T cells: A common basis between tumor immunity and autoimmunity. *J Immunol* 163:5211–5218.
6. Wolf AM, et al. (2003) Increase of regulatory T cells in the peripheral blood of cancer patients. *Clin Cancer Res* 9:606–612.
7. Curiel TJ, et al. (2004) Specific recruitment of regulatory T cells in ovarian carcinoma fosters immune privilege and predicts reduced survival. *Nat Med* 10:942–949.
8. Petersen RP, et al. (2006) Tumor infiltrating Foxp3+ regulatory T-cells are associated with recurrence in pathologic stage I NSCLC patients. *Cancer* 107:2866–2872.
9. Shang B, Liu Y, Jiang SJ, Liu Y (2015) Prognostic value of tumor-infiltrating FoxP3+ regulatory T cells in cancers: A systematic review and meta-analysis. *Sci Rep* 5:15179.
10. Miyara M, et al. (2009) Functional delineation and differentiation dynamics of human CD4+ T cells expressing the FoxP3 transcription factor. *Immunity* 30:899–911.
11. Wing JB, et al. (2017) A distinct subpopulation of $CD25^-$ T-follicular regulatory cells localizes in the germinal centers. *Proc Natl Acad Sci USA* 114:E6400–E6409.
12. Saito T, et al. (2016) Two FOXP3(+)CD4(+) T cell subpopulations distinctly control the prognosis of colorectal cancers. *Nat Med* 22:679–684.
13. Sugiyama D, et al. (2013) Anti-CCR4 mAb selectively depletes effector-type FoxP3+ CD4+ regulatory T cells, evoking antitumor immune responses in humans. *Proc Natl Acad Sci USA* 110:17945–17950.
14. Shevach EM (2009) Mechanisms of foxp3+ T regulatory cell-mediated suppression. *Immunity* 30:636–645.
15. Wing K, et al. (2008) CTLA-4 control over Foxp3+ regulatory T cell function. *Science* 322:271–275.
16. Qureshi OS, et al. (2011) Trans-endocytosis of CD80 and CD86: A molecular basis for the cell-extrinsic function of CTLA-4. *Science* 332:600–603.
17. Hodi FS, et al. (2010) Improved survival with ipilimumab in patients with metastatic melanoma. *N Engl J Med* 363:711–723.
18. Robert C, et al. (2011) Ipilimumab plus dacarbazine for previously untreated metastatic melanoma. *N Engl J Med* 364:2517–2526.
19. Bulliard Y, et al. (2013) Activating Fc γ receptors contribute to the antitumor activities of immunoregulatory receptor-targeting antibodies. *J Exp Med* 210:1685–1693.
20. Simpson TR, et al. (2013) Fc-dependent depletion of tumor-infiltrating regulatory T cells co-defines the efficacy of anti-CTLA-4 therapy against melanoma. *J Exp Med* 210:1695–1710.
21. Selby MJ, et al. (2013) Anti-CTLA-4 antibodies of IgG2a isotype enhance antitumor activity through reduction of intratumoral regulatory T cells. *Cancer Immunol Res* 1: 32–42.
22. Nimmerjahn F, Ravetch JV (2008) Fcgamma receptors as regulators of immune responses. *Nat Rev Immunol* 8:34–47.
23. Mimoto F, et al. (2013) Novel asymmetrically engineered antibody Fc variant with superior FcγR binding affinity and specificity compared with afucosylated Fc variant. *MAbs* 5:229–236.
24. Maeda Y, et al. (2014) Detection of self-reactive $CD8^+$ T cells with an anergic phenotype in healthy individuals. *Science* 346:1536–1540.
25. Gnjatic S, et al. (2006) NY-ESO-1: Review of an immunogenic tumor antigen. *Adv Cancer Res* 95:1–30.
26. Arce Vargas F, et al.; Melanoma TRACERx Consortium; Renal TRACERx Consortium; Lung TRACERx Consortium (2017) Fc-optimized anti-CD25 depletes tumor-infiltrating regulatory T cells and synergizes with PD-1 blockade to eradicate established tumors. *Immunity* 46:577–586.
27. Arce Vargas F, et al.; TRACERx Melanoma; TRACERx Renal; TRACERx Lung consortia (2018) Fc effector function contributes to the activity of human anti-CTLA-4 antibodies. *Cancer Cell* 33:649–663.e4.
28. Bulliard Y, et al. (2014) OX40 engagement depletes intratumoral Tregs via activating FcγRs, leading to antitumor efficacy. *Immunol Cell Biol* 92:475–480.
29. Romano E, et al. (2015) Ipilimumab-dependent cell-mediated cytotoxicity of regulatory T cells ex vivo by nonclassical monocytes in melanoma patients. *Proc Natl Acad Sci USA* 112:6140–6145.
30. Walker LSK, Sansom DM (2011) The emerging role of CTLA4 as a cell-extrinsic regulator of T cell responses. *Nat Rev Immunol* 11:852–863.
31. Linsley PS, et al. (1996) Intracellular trafficking of CTLA-4 and focal localization towards sites of TCR engagement. *Immunity* 4:535–543.
32. Egen JG, Allison JP (2002) Cytotoxic T lymphocyte antigen-4 accumulation in the immunological synapse is regulated by TCR signal strength. *Immunity* 16:23–35.
33. Ko K, et al. (2005) Treatment of advanced tumors with agonistic anti-GITR mAb and its effects on tumor-infiltrating $Foxp3^+CD25^+CD4^+$ regulatory T cells. *J Exp Med* 202: 885–891.
34. Prieto PA, et al. (2012) CTLA-4 blockade with ipilimumab: Long-term follow-up of 177 patients with metastatic melanoma. *Clin Cancer Res* 18:2039–2047.
35. Mei HE, Leipold MD, Schulz AR, Chester C, Maecker HT (2015) Barcoding of live human peripheral blood mononuclear cells for multiplexed mass cytometry. *J Immunol* 194:2022–2031.